Molecular Cancer

CORRESPONDENCE

Open Access

Assessment of SWI/SNF chromatin remodeling complex related genes as potential biomarkers and therapeutic targets in pan-cancer

Kai Zhuang[1†], Lishan Wang[1†], Chengyu Lu[1†], Zhiping Liu[2†], Dongli Yang[1], Hao Zhong[1], Jiami Zou[2], Aamir Fahira[1], Jiaojiao Wang[2*] and Zunnan Huang[1*]

Abstract

Recent research has uncovered a surprisingly high occurrence of aberrant expression and mutations in the genes that encode subunits of the SWI/SNF chromatin-remodeling complexes (SCRC). Nevertheless, the carcinogenic effects of aberrant expression and mutations in SWI/SNF genes have only been acknowledged in recent times, resulting in a comparatively limited understanding of these modifications. In this study, we comprehensively analyzed the expression difference, somatic mutation, potential biological pathways, stromal or immune cell infiltration, and drug sensitivity of SCRC-related genes (SCRGs) in pan-cancer. Furthermore, the evolutionary trend, prognostic signature, and immunotherapy response of SCRGs in kidney renal clear cell carcinoma (KIRC) were also evaluated. The expression of SCRGs was changed in 13 out of 14 tumor types, strongly linked to prognosis, and mutated in 30.9% of tumor patients. SCRGs were also closely associated with immune-related pathways and tumor metastasis pathways. The expression of SCRGs was positively associated with the immune score or stromal score but negatively correlated with Tumor purity. Three potential drugs (FK866, Ispinesib mesylate, and WZ3105) were identified to target the SCRGs. In KIRC, scRNA-seq analysis showed that the enrichment of SCRC and the communication frequency with immune cells were significantly declined during tumor cell progression. A prognostic signature was constructed in KIRC and was effective in predicting the prognosis for KIRC. Aberrant expression of eleven prognostic genes identified from the KIRC prognostic signature and the cytotoxicity of FK866 and Ispinesib mesylate to KIRC were verified by qRT-PCR and CCK-8 assay, respectively. Our study identified SCRGs as potential biomarker and therapeutic targets, providing new insights into SCRC for tumor-targeted therapy.

Keywords SWI/SNF, Mutation, KIRC, Prognosis, Immunotherapy, Pan-cancer

†Kai Zhuang, Lishan Wang, Chengyu Lu and Zhiping Liu contributed equally to this work.

*Correspondence:
Jiaojiao Wang
jjwang@jnu.edu.cn
Zunnan Huang
zn_huang@gdmu.edu.cn

[1]Key Laboratory of Big Data Mining and Precision Drug Design of Guangdong Medical University, Key Laboratory of Computer-Aided Drug Design of Dongguan City, Key Laboratory for Research and Development of Natural Drugs of Guangdong Province, School of Pharmacy, Guangdong Medical University, Dongguan, Guangdong Province 523808, PR China
[2]State Key Laboratory of Bioactive Molecules and Druggability Assessment, College of Pharmacy, Jinan University, Guangzhou, Guangdong Province 510632, PR China

Introduction

The SWI/SNF chromatin remodeling complex (SCRC) is a subfamily of ATP-dependent chromatin remodeling proteins that play broad roles in regulating gene expression through the modification of chromatin structure [1]. The SCRC is composed of two ATPases, SMARCA4 and SMARCA2, along with other core subunits, including SMARCB1, PBRM1, SMARCC1, ARID1A, ARID1B, and others [2].

Emerging studies have indicated that there is a high prevalence of mutations in the genes responsible for encoding the subunits of the SWI/SNF complex in multiple cancer types [3]. SMARCB1 is silenced by biallelic mutations in almost all instances of rhabdoid tumors, which typically develop in children under the age of 3 with a notably unfavorable prognosis [4]. The presence of the PBRM1 mutation, in addition to the VHL mutation which is a hallmark of kidney clear cell renal carcinoma (KIRC), contributes to the development of bilateral and multifocal clear cell kidney malignancies [5]. SMARCA4 has been identified as frequently mutated in lung cancer and has driven cancer progress, leading to the development of highly sophisticated undifferentiated malignancies and an elevated occurrence of metastasis [6]. Recently, the first small-molecule inhibitor (Tazemetostat) of EZH2 exhibited a promising safety profile and demonstrated anticancer effectiveness in patients diagnosed with B-cell non-Hodgkin lymphoma and INI1 or SMARCA4-negative tumors [7]. EZH2 is a methyltransferase, and its enzyme activity is tightly and reversely regulated by the SWI/SNF complex [8]. Thus, impeding mutations associated with the SWI/SNF complex represent a promising therapeutic strategy for mutation-addicted cancers. Despite the fact that aberrant expression and mutations in the SWI/SNF complex are prevalent in cancers and a few mutations have been investigated in certain cancer types, the landscape of the SWI/SNF complex in pan-cancer is still in need of additional refinement and mapping.

Results

Investigation of disparities in gene expression, genetic alterations, immune infiltration, effect on signaling pathways, and responsiveness to drugs in SCRGs

The materials and methods are thoroughly documented in the Supplementary Materials section. The cancer types with abbreviations and twenty-nine SWI/SNF-related genes identified for the analysis are listed in Sup. Tables 1 and 2, respectively. The flow chart of this study is shown in Sup. Figure 1.

The SCRGs mRNA levels exhibited considerable fluctuations in 13 tumor types, especially in LUSC (24/29), KIRC (21/29), BRCA (20/29), LIHC (20/29), and THCA (20/29) (Fig. 1A). Specifically, most SCRGs had significant differential expression across BRCA, GBM, KIRC, LUAD, LUSC, and STAD tumor subtypes (Fig. 1B). Furthermore, the survival analysis employing Cox proportional risk regression models demonstrated a substantial correlation between the expression of SCRGs and the prognoses of several types of tumors, particularly LGG and KIRC (Sup. Table 3 and Fig. 1C). Besides expression profile, the top 5 mutation frequencies of SCRGs were ARID1A (26%), PBRM1 (13%), ARID2 (13%), SMARCA4 (12%), and ARID1B (11%), and the top 10 mutated SCRGs in total were present in 69.73% (2209/3168) of tumor patients (Fig. 1D). All the mutated SCRGs were detected in UCEC and SKCM, while PCPG, TGCT, LAML, KICH, and UVM harbored much fewer mutations (Sup. Figure 2). Nevertheless, the occurrence of simultaneous mutations in more than one subunit is infrequent. One probable explanation is that in such cases, the patient's chances of survival and prognosis may be significantly diminished (Sup. Figure 3). Substantial copy number variations (CNVs) of SCRGs were also noticed in most tumor types (Sup. Figure 4). The expression of SCRGs in most tumor types showed a positive correlation with CNV levels, especially BRCA, LUSC, and OV (Sup. Figure 5). In contrast, for LAML, DLBC, and THCA, the expression of SCRGs did not exhibit a significant association with CNV levels (Sup. Figure 5). Intriguingly, SCRGs correlated positively with tumor mutation burden (TMB) in SARC but negatively in seven other cancer types (PRAD, LUSC, LIHC, LUAD, ACC, PAAD, and CESC) (Sup. Figure 6 A). Similarly, SCRGs were positively correlated with microsatellite instability (MSI) in COAD but negatively in ten other cancer types (LUSC, HNSC, LUAD, PRAD, STAD, LIHC, SKCM, PCPG, OV, and TGCT) (Sup. Figure 6B).

Immune infiltration of malignancies correlates strongly with clinical outcomes [9]. The expression of SCRGs was positively correlated with stromal score, immune score, and ESTIMATE scores while negatively correlated with tumor purity (Fig. 1E). Immune cell infiltration showed a positive association between SCRGs and immune-inflammatory cells such as CD8 naïve cells, B cells, and CD4 T cells, while displaying a negative association with immunosuppressive cells such as macrophages, DC, and NK cells (Fig. 1F). SCRGs were positively correlated with chemokine genes in distinct tumor types, showing that SCRGs also promote chemokine expression (Sup. Figure 7).

In terms of signaling pathway regulation, our analyses showed that the TNFα signaling via NF-κB, P53 pathway, IL-2/STAT5 signaling, IL-6/JAK-STAT3 signaling, inflammatory response, epithelial-mesenchymal transition, and apoptosis pathways were significantly activated, and the oxidative phosphorylation, Myc, G2M checkpoint, and E2F pathways were significantly inhibited in multiple cancer types (Fig. 1G). Lastly, drug sensitivity

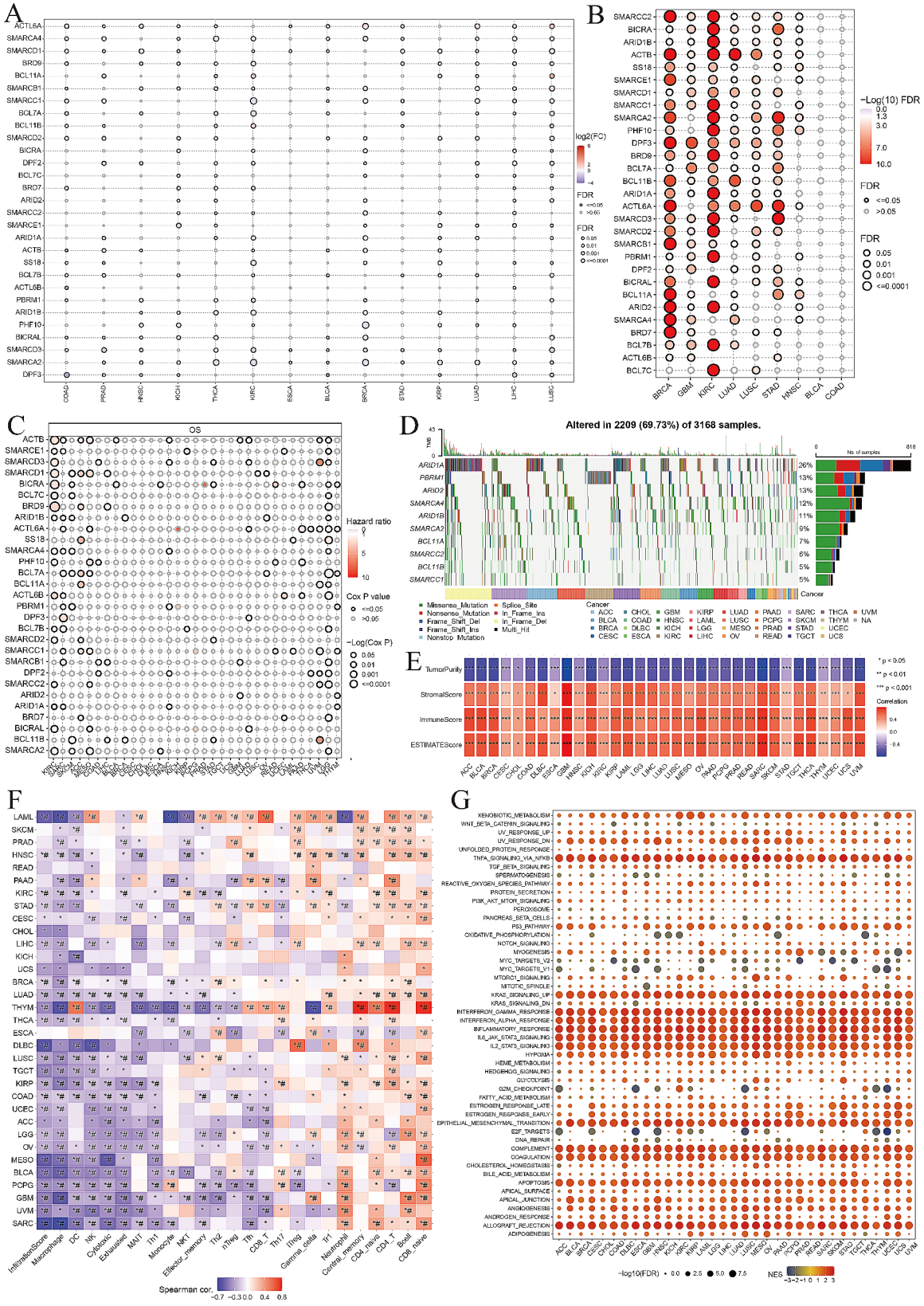

Fig. 1 (See legend on next page.)

(See figure on previous page.)

Fig. 1 Gene expression, genetic alteration, immune infiltration, effect on the signaling pathway, and responsiveness to drugs of SWI/SNF complex-related genes (SCRGs). (**A**) Differential expression analysis of SCRGs in 14 tumor types that meet the inclusion criteria with more than 10 available normal tissues adjacent to the tumors, represented by log2(FC) and false discovery rate (FDR) values. The color scale represents log2(FC) values, with red indicating upregulation (log2 (FC) > 0) and blue indicating downregulation (log2(FC) < 0). (**B**) Differential expression analysis of SCRGs in different tumor subtypes. The redder the color, the higher the FDR value. (**C**) Prognostic survival analysis of SCRGs for 33 tumor types. The Hazard Ratio (HR) value is indicated by the color, with a higher HR value in redder colors. (**D**) The waterfall plot shows the mutation distribution and types of the top 10 mutated genes in SCRGs. (**E**) Spearman correlation analysis of the ESTIMATE score and single-sample gene set enrichment analysis (ssGSEA) score: positive correlation in red, negative correlation in blue. *$P < 0.05$, **$P < 0.01$, ***$P < 0.001$. (**F**) Spearman correlation analysis of gene set variation analysis (GSVA) score and immune cell infiltration. *$P < 0.05$; #FDR < 0.05. (**G**) Gene set enrichment analysis (GSEA) of SCRGs in pan-cancer. The size of the circles represents the FDR value for each enrichment cancer pathway, and the color represents the normalized enrichment score (NES) for each enrichment cancer pathway

prediction showed that three potential drugs (WZ3105, Ispinesib mesylate, and FK866) exhibited high sensitivity to the expression of the majority of SCRGs (Sup. Figure 8).

Tumor cell evolution and construction of the prognostic signature of SCRGs in KIRC

Based on our above analyses, KIRC was identified as one of the two tumor types, along with LUSC, that had the highest number of altered SCRGs (Fig. 1A). Thus, KIRC was chosen as a representative tumor type for the following analysis. Nine cell types and ten subpopulations from the single-cell RNA sequencing (scRNA-seq) data (GSE159115) in KIRC were further identified (Sup. Figure 9A-B). Enrichment analysis revealed that SCRGs were highly enriched in tumor cell clusters 1, 3, and 7 and less enriched in clusters 0, 4, and 9 (Fig. 2A and Sup. Figure 9B-C). Pseudotime analysis showed that KIRC tumor cells evolve into three branches, starting in state 1 (which mainly consists of clusters 1, 3, and 7) and going on to state 3 (which mainly consists of clusters 2, 5, and 6) and state 2 (which mainly consists of clusters 0, 2, 4, 8, and 9) (Fig. 2B and Sup. Figure 9D-E). The enrichment level of SCRGs in state 1 was significantly higher than the other two branches, while state 3 was higher than state 2 (Fig. 2C). The cellular communication analysis also revealed that tumor cells exhibiting elevated levels of SCRGs displayed a greater propensity for intercellular communication with DC, monocyte, and macrophage immune cells (Sup. Figure 9F-G). Additionally, the communication between tumor cells with high and low SCRGs enrichment and immune cells showed significant differences in ligand-receptor pairings (Sup. Figure 10).

The abnormal pattern of SCRGs in tumors is strongly correlated with prognosis. Based on the 21 SCRGs that were differentially expressed in KIRC (Sup. Table 4), a prognostic signature for KIRC consisting of 11 screened prognostic SCRGs was developed by multivariate Cox regression analysis (Sup. Table 5). This signature produced risk assessments for each individual and categorized them as either "high-risk" or "low-risk" based on the median results. The ROC curves demonstrated the reliability of the prognostic signature, as indicated by the AUC values of 0.75, 0.75, and 0.85 for 1, 5, and 10-year survival, respectively (Fig. 2D). The Kaplan-Meier (K-M) survival curves demonstrated that low-risk patients survived longer than high-risk patients by the log-rank test (Fig. 2E). To further improve KIRC prognosis, a nomogram was created to combine risk group and clinical phenotype, such as age, laterality, M stage, T stage, and stages (I - IV) (Fig. 2F). Next, the nomogram employing these prognostic parameters revealed that laterality, age, risk group, T stage, and stages are important for KIRC overall survival (OS) prediction (Fig. 2G). The calibration plots for internal validation of the line graphs revealed excellent agreement between predicted probabilities and actual observations of 1, 5, and 10-year OS (Fig. 2H). The predictive accuracy of the prognostic signature was enhanced by the nomogram, as indicated by AUC values of 0.87, 0.82, and 0.85 for the 1-year, 5-year, and 10-year, respectively (Fig. 2I). The high-risk group had elevated levels of LAG3, CTLA4, CD28, PDCD1, LMTK3, CD40, and TIGIT immune checkpoints, whereas there were no differences observed in SIGLEC15, HAVCR2, PDCD1LG2, and CD274 (Fig. 2J). TIDE scores also showed that the high-risk group had higher scores, which indicated more immune escape and a worse immunotherapy response, than the low-risk group (Fig. 2K).

Experimental validation

The transcript level of 11 prognostic genes identified from the KIRC prognostic signature was evaluated in two KIRC tumor cell lines (786-O and Caki-1) and normal human renal proximal tubular epithelial cells (HK-2) by using quantitative reverse transcription-polymerase chain reaction (qRT-PCR) (Sup. Table 6). Concisely, compared to HK-2 cells, SMARCC2 and SMARCD1 remained unchanged in 786-O cells but were still upregulated in Caki-1 cells ($P < 0.001$). Furthermore, upregulation of the other four prognostic genes (ACTB, BRD9, BCL11A, and BCL7B) and downregulation of all five prognostic genes (SMARCA2, PHF10, ARID1B, BCL7A, and SMARCC1) were observed in both 786-O and Caki-1 cells (Sup. Fig. 11A), which were consistent with our calculations.

In addition, we evaluated the cytotoxic effects of two commercially available drugs, FK866 and Ispinesib

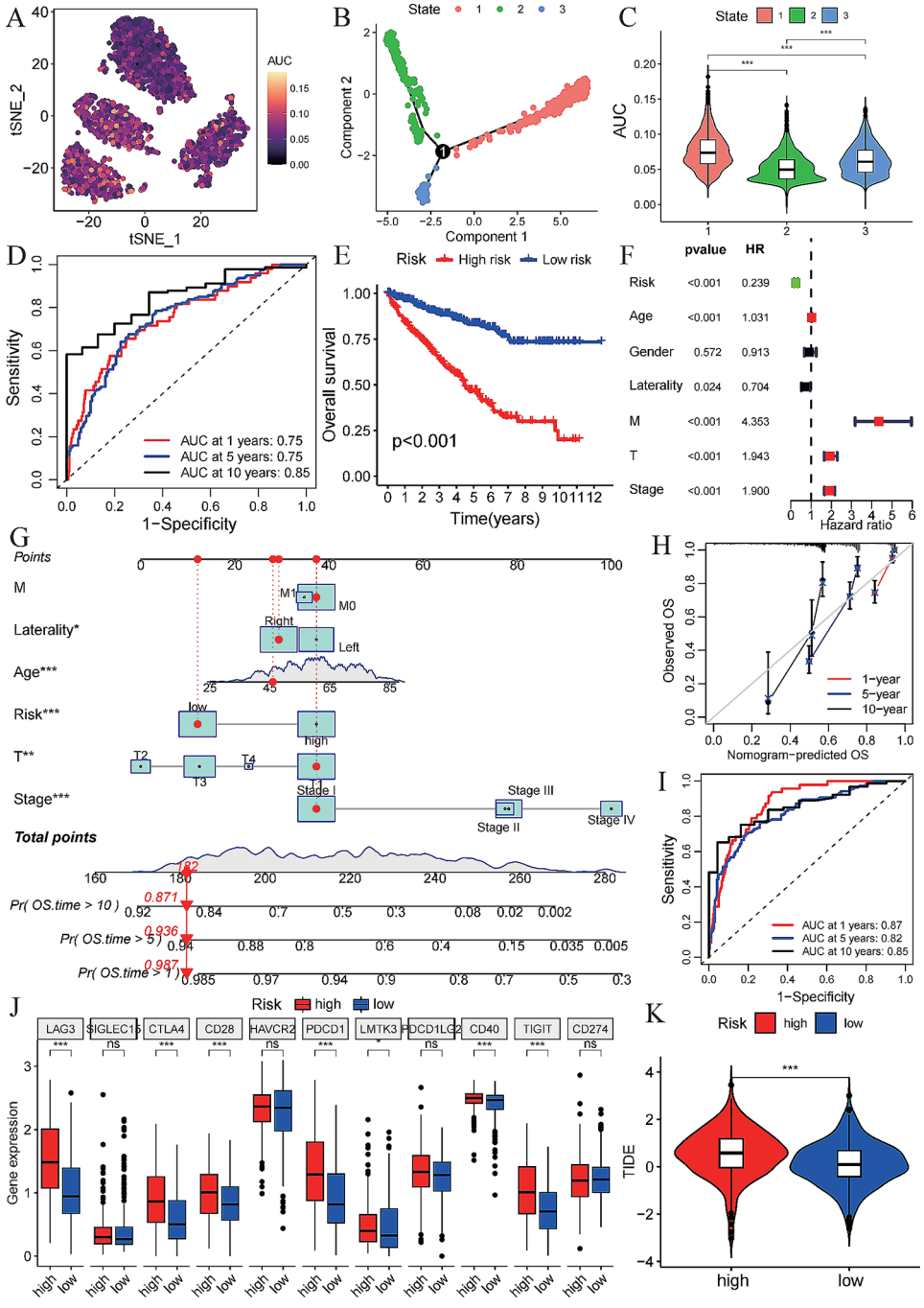

Fig. 2 Tumor cell evolution and construction of the prognostic signature of SCRGs in KIRC. (**A**) The T-distributed Neighbor Embedding (tSNE) plots visually illustrate the enrichment levels of SCRGs in each cell. The area under the curve (AUC) value represents SCRGs' enrichment levels. The brighter the color, the higher the AUC. (**B**) The pseudotime trajectory plot for KIRC was constructed based on risk scores and clinical phenotypes. (**C**) Violin plots indicate the enrichment levels of SCRGs for the three proposed chronological branches. *$P < 0.05$, **$P < 0.01$, ***$P < 0.001$. (**D**) Receiver operating characteristic (ROC) curves for prognostic signature. (**E**) Survival curves for prognostic signature. (**F**) Forest plots of risk groups and clinical phenotypes (**G**) A nomogram for KIRC was constructed based on risk scores and clinical phenotypes. (**H**) Calibration curves of internal validation of the nomogram. (I) ROC curves for the nomogram at 1, 5, and 10 years of prediction. (**J**) Comparison of the expression of immune checkpoint genes in high- and low-risk groups. (**K**) Comparison of tumor immune dysfunction and exclusion (TIDE) scores in high- and low-risk groups

mesylate, using cell counting kit-8 (CCK-8) assays. Both FK866 and Ispinesib mesylate exhibited cytotoxic effects on 786-O and Caki-1 cells. Notably, Ispinesib mesylate showed strong cytotoxicity to the two tumor cell lines in a dose-dependent manner (Sup. Fig. 11B). This finding suggests that drug prediction analysis in this study is

reliable and provides an effective way to find personalized drug selection in clinical practice.

Conclusion

This study represents the initial attempt to perform a thorough pan-cancer examination of SCRGs, which have demonstrated potential as therapeutic targets and autonomous prognostic epigenetic biomarkers. The analysis uncovers the extent of mutational and copy number variations in SCRGs across a diverse array of cancers. Our analyses indicate a possible strong association between the SWI/SNF chromatin remodeling complex and anticancer drugs. The single-cell RNA sequencing investigation demonstrated a strong correlation between SCRC and the phenomenon of cancer cell evolution in KIRC. Moreover, a novel set of eleven-gene-signature was developed specifically for KIRC. Furthermore, in KIRC tumor cells, the transcript level of eleven prognostic genes and the cytotoxicity of potential drugs (FK866 and Ispinesib mesylate) were also validated using qRT-PCR and CCK-8 assays. In conclusion, we provide new information regarding the putative anti-tumor mechanisms linked to the SWI/SNF chromosomal complex, warranting further investigation and confirmation.

Supplementary Information

The online version contains supplementary material available at https://doi.org/10.1186/s12943-024-02015-w.

Supplementary Material 1

Acknowledgements
Not applicable.

Author contributions
K.Z.: Conceptualization, Data curation, Data analysis, Writing - Original draft; L.W.: Formal analysis, Writing - Review & Editing, Visualization, Writing - Original draft; C.L.: Writing - Review & Editing, Supervision; Z.L.: Writing - Review & Editing, Supervision, experimental validation; D.Y.: Data analysis, Writing - Review & Editing; H.Z.: Data analysis; J.Z.: Writing - Review & Editing, experimental validation; A.F.: Writing - Review & Editing; J.W.: Data analysis, Writing - Review & Editing; Funding acquisition; Z.H.: Conceptualization, Writing - Review & Editing, Supervision, Funding acquisition.

Funding
This research was funded by the National Natural Science Foundation of China (Grant No. 82203304) and Key Discipline Construction Project of Guangdong Medical University (Grant No. 4SG23004G).

Data availability
The datasets presented in this study can be found in online repositories. The names of the repository/repositories and accession number(s) can be found in the article/Supplementary Material.

Declarations

Ethics approval and consent to participate
Not applicable.

Consent for publication
Not applicable.

Competing interests
The authors declare that they have no competing interests.

Received: 17 January 2024 / Accepted: 3 May 2024
Published online: 27 August 2024

References

1. Ahmad K, Brahma S, Henikoff S. Epigenetic pioneering by SWI/SNF family remodelers. Mol Cell. 2024;84:194–201.
2. Mashtalir N, D'Avino AR, Michel BC, Luo J, Pan J, Otto JE, Zullow HJ, McKenzie ZM, Kubiak RL, St Pierre R, et al. Modular Organization and Assembly of SWI/SNF family chromatin remodeling complexes. Cell. 2018;175:1272–e12881220.
3. Mittal P, Roberts CWM. The SWI/SNF complex in cancer - biology, biomarkers and therapy. Nat Rev Clin Oncol. 2020;17:435–48.
4. Roberts CW, Biegel JA. The role of SMARCB1/INI1 in development of rhabdoid tumor. Cancer Biol Ther. 2009;8(5):412-6.
5. Nargund AM, Pham CG, Dong Y, Wang PI, Osmangeyoglu HU, Xie Y, Aras O, Han S, Oyama T, Takeda S, et al. The SWI/SNF protein PBRM1 restrains VHL-Loss-driven Clear Cell Renal Cell Carcinoma. Cell Rep. 2017;18:2893–906.
6. Concepcion CP, Ma S, LaFave LM, Bhutkar A, Liu M, DeAngelo LP, Kim JY, Del Priore I, Schoenfeld AJ, Miller M, et al. Smarca4 inactivation promotes lineage-specific Transformation and early metastatic features in the lung. Cancer Discov. 2022;12:562–85.
7. Italiano A, Soria JC, Toulmonde M, Michot JM, Lucchesi C, Varga A, Coindre JM, Blakemore SJ, Clawson A, Suttle B, et al. Tazemetostat, an EZH2 inhibitor, in relapsed or refractory B-cell non-hodgkin lymphoma and advanced solid tumours: a first-in-human, open-label, phase 1 study. Lancet Oncol. 2018;19:649–59.
8. Drosos Y, Myers JA, Xu B, Mathias KM, Beane EC, Radko-Juettner S, Mobley RJ, Larsen ME, Piccioni F, Ma X, et al. NSD1 mediates antagonism between SWI/SNF and polycomb complexes and is required for transcriptional activation upon EZH2 inhibition. Mol Cell. 2022;82:2472–e24892478.
9. Fridman WH, Zitvogel L, Sautes-Fridman C, Kroemer G. The immune contexture in cancer prognosis and treatment. Nat Rev Clin Oncol. 2017;14:717–34.

Publisher's Note